*Int. J. Electrochem. Sci.*, 11 **(2016)** 8471 – 8485, doi: 10.20964/2016.10.36

**International Journal of ELECTROCHEMICAL SCIENCE**
www.electrochemsci.org

# Optimization of 4- chlorophenol Oxidation by Manganese Ferrite Nanocatalyst with Response Surface Methodology

*Ghasem Hassani*[1], *Afshin Takdastan*[1], *Mehrorang Ghaedi*[2], *Gholamreza Goudarzi*[1],
*Abdolkazem Neisi*[1], *Ali Akbar Babaei*[3, 1, *]

[1] Department of Environmental Health Engineering, School of Public Faculty, Ahvaz Jundishapur University of Medical Sciences, Ahvaz, Iran
[2] Chemistry Department, Yasouj University, Yasouj 75914-35, Iran
[3] Environmental Technologies Research Center (ETRC), Ahvaz Jundishapur University of Medical Sciences, Ahvaz, Iran
[*] E-mail: babaei–a@ajums.ac.ir

*Received:* 23 April 2016 / *Accepted:* 19 July 2016 / *Published:* 6 September 2016

---

In this study, manganese ferrite ($MnFe_2O_4$) was prepared by a co-precipitation method and used as a magnetic catalyst for the degradation of 4-chlorophenol in Advanced Oxidation Process (AOP). In order to find the best operating condition in 4-Chlorophenol degradation in Fenton process, adopted response surface methodology (RSM) and Central composite factorial design (CCD) were used to investigate the effective parameters such as pH, catalyst and $H_2O_2$ dosage, 4-Chlorophenol concentration, and process time. Characterization of synthesized manganese ferrite by field emission scanning electron microscopy (FESEM), energy dispersive spectroscopy (EDS), and Vibrating Sample Magnetometer (VSM) explained the porous structure of super-para magnetic $MnFe_2O_4$ and showed that Fe, O and Mn are the dominant elements in the composite with weight percentages of 47.20, 28.40 and 24.40%, respectively; and also, the result of powder X-ray diffractometer (XRD) confirmed the presence of single phase $MnFe_2O_4$ with a face-centered cubic structure. Degradation efficiency was observed through an oxidation process indicated that 4-Chlorophenol could be 93% reduced by $MnFe_2O_4$ within 60min. Furthermore, optimum pH, $H_20_2$, and catalyst were 4.24, 0.07 mol. $L^{-1}$, and 0.72 g. $L^{-1}$, respectively. Second-order polynomial equation for the degradation efficiency of 4-chlorophenol expressed the relation between response variable and the test variables. P-Value of the model (<0.0001) showed that the model was suitable for this experiment.

---

**Keywords:** manganese ferrite; Advanced Oxidation Process; 4-chlorophenol; central composite; ElectroFenton

## 1. INTRODUCTION

Chlorophenols are a group of chemicals resulted from adding chlorines to phenol molecule. Phenolic compounds are toxic and water soluble which are being continuously released to the environment through industrial and household activities [1-4]. Phenolic wastewaters are produced from resin manufacturing, building materials, automobile, paper, textile, artificial rubber, pharmaceutical, and oil industry [2, 5, 6]. These compounds cause unsightly taste and odor in drinking water and can exert negative effects on different biological processes [7]. Removal of chlorinated phenolic compounds is of high importance due to their high toxicity at low concentrations. Phenols and its chlorinated compounds are toxic for human beings as well as aquatic life. Treatment of these compounds is difficult or near to impossible by conventional biological treatment processes.

lately, different technologies have been used to remove chlorophenol from aqueous solutions, such as adsorption [8-10], chemical reduction treatment using zero-valent iron [11], electrochemical oxidation [12], catalytic wet oxidation [13, 14], and radiation-induced degradation [15, 16].

Advanced oxidation processes (AOPs) are more desirable than the physical and biological methods because they mineralize toxic organic material, while the physical methods produce secondary waste and biological processes are time consuming [17, 18]. Between the AOP methods, Fenton processes have been widely used due to their good performance, cost-effectiveness, simplicity of technology, and low toxicity of the reagents [19]. Yuan and Lu [20] worked on removing chlorophenol using Electro-Fenton process; they observed that the addition of tiny amounts of $Fe^{2+}$ or $Fe^{3+}$ significantly accelerate the rate of the process.

In addition, the destruction of color using Fenton's reagent has been reported in the literature and shown promising results [21-23]. The Fenton's process is a promising advanced oxidation process (AOP) that could mineralize high and low level organic polluted wastewater [24]. In this process, hydroxyl radicals ($HO^\bullet$) are derived by the reaction of ferrous ions ($Fe^{+2}$) and hydrogen peroxide ($H_2O_2$) (Eq. 1). Ferrous ions can be restored by Eqs. (2) and (3). It should be noted that applying magnetic oxides not only promote the recovery of ferrous ions (Eq. 4) as Fenton-like process but also generate hydroxyl radicals by equation (5).

$$Fe^{2+} + H_2O_2 \rightarrow Fe^{3+} + HO^\bullet + HO^- \qquad (1)$$

$$Fe^{3+} + H_2O_2 \rightarrow Fe^{2+} + H^+ + HOO^\bullet \qquad (2)$$

$$Fe^{3+} + HOO^\bullet \rightarrow Fe^{2+} + H^+ + O_2 \qquad (3)$$

$$[Fe(OH)]^{2+} + hv \rightarrow Fe^{2+} + HO^\bullet \qquad (4)$$

$$H_2O_2 + hv \rightarrow 2HO^\bullet \qquad (5)$$

Application of conventional Fenton process is limited by its narrow working pH range and the accumulation of ferric oxide sludge; in other words, there is a possibility to have secondary pollution in the reaction media. On the other hand, in homogeneous Fenton process, the ferrous ions can quench the hydroxyl radicals resulting in the reduction of the efficiency of the process [25]. The heterogeneous catalysts remain stable and have long life time and also can be regenerate easily. Furthermore, in heterogeneous Fenton process most amount of iron or any metal ion that used as catalyst remains in solid phase and the metal ions concentration in solution are increased in very low extent and also, these metal ions can be easily separated from the solution [26].

$$Fe^{2+} + OH^{\bullet} \rightarrow Fe^{3+} + OH^{-} \qquad (6)$$

To reduce the hydroxyl radicals quenching, the ferrous ion dosage should be kept at low levels. To this aim, the heterogeneous Fenton process as one of the new AOP methods has been considered by researchers [27]. Heterogeneous Fenton process has some advantages such as a wider working pH range, reusability of catalyst and it does not produce any sludge and secondary pollution.

Both Fenton reagents ($H_2O_2$ and $Fe^{2+}$) could be generated in situ by electrochemical process that this process is called electro-Fenton. In this process there is no need to add chemicals to the reaction media. Many researchers have been studied Electro-Fenton processes in removal of different organic pollutant[28, 29]. In this process, oxygen diffused to solution phase in first step then attracted on the cathode surface and finally the process is completed by hydrogen peroxide production in electrochemical reactions [30, 31]. in this process hydrogen peroxide and Ferrous ions ($Fe^{2+}$) was simultaneously produced by electrochemical reduction of oxygen molecules and ferric ion in surface of cathode [32]. These reactions of hydrogen peroxide production and destruction described as below [33]:

$$2H_2O \rightarrow O_2 + 4H^{+} + 4e^{-} \qquad (7)$$

$$O_2 + 4H^{+} + 4e^{-} \rightarrow H_2O_2 \qquad (8)$$

$$Fe^{3+} + e^{-} \rightarrow Fe^{2+} \qquad (9)$$

$$Fe^{2+} + H_2O_2 \rightarrow Fe^{3+} + OH^{\bullet} + HO^{-} \qquad (10)$$

Catalytic activity of spinel ferrites containing transition metal ions have been investigated in the Fenton reaction through cyclic electron transfer process [27]. Various factors, including particle size, redox properties of metal ions and their distribution among the tetrahedral and octahedral co-ordination sites influence on the catalytic activity of spinel ferrites [27]. Spinel ferrites have better catalytic activities, compared to single component metal oxide such as $Fe_3O_4$ duo to its greater stability towards acids [34]. In addition, nano $MnFe_2O_4$ with paramagnetic behavior has more specific surface area than $Fe_3O_4$ has. Hence, the $MnFe_2O_4$ can be used to produce hydroxyl radical from $H_2O_2$ and easily separated by applying an external magnetic field at the end of the process [35, 36].

In the $MnFe_2O_4$, the catalyst transition of $Fe^{2+}$ to $Fe^{3+}$ and $Mn^{2+}$ to $Mn^{3+}$ generates highly active hydroxyl radicals in the presence of $H_2O_2$; besides, recycling the ions is performed by produced combination and intermediate [36]. Schematic view of the heterogeneous Fenton reactions using $MnFe_2O_4$ is shown in Fig. 1. In this research Fenton like process in the presence of manganese ferrite was used to remove 4- chlorophenol. Manganese ferrite nanoparticles were synthesized and characterized by chemical precipitation methods. In this study, we investigated the effect of various parameters, including pH, catalyst dosage, initial 4-chlorophenol concentration, processing time and $H_2O_2$ dosage on the degradation of 4-chlorophenol as organic pollutant from the aqueous solution. Finally, 4-chlorophenol degradation removal in optimum condition was comprised with the removal efficiency in ElectroFenton and hybrid process.

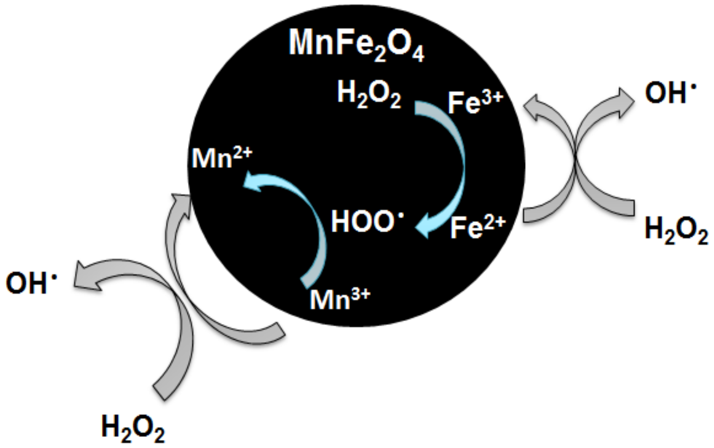

**Figure 1.** Schematic view of heterogeneous $MnFe_2O_4$ Fenton reactions

## 2. EXPERIMENTAL SECTION

### *2.1. Materials*

The Iron (III) chloride ($FeCl_3$), Manganese (II) chloride ($MnCl_2$), Sodium hydroxide (NaOH), sulfuric acid ($H_2SO_4$), Potassium ferricyanide ($K_3Fe\ (CN)_6$), and ethanol were purchased from Merck Company. Hydrogen peroxide ($H_2O_2$) and 4-Aminoantipyrine ($C_{11}H_{13}N_3O$), phosphate buffer saline 0.1M, and 4-chlorophenol were purchased from Sigma Company, and were used without any purification. Double distilled water was used to prepare stock solutions and samples.

### *2.2. Catalyst synthesis and characterization*

$MnFe_2O_4$ nanocatalyst was synthesis by co-precipitation method as described below. First by dissolving $FeCl_3$ and $MnCl_2$ in their stoichiometric ratio in 50cc double distilled water, metal salt solutions were prepared. Then 1 gram sodium hydroxide dissolved in 50cc Double distilled water. In next step, metal salt solutions were transferred to the under vigorous stirring and nitrogen atmosphere teflon. After 30 min of stirring of the mixture in 80˚C, NaOH solution was added to the mixed solutions in 30 minutes drop-by-drop. The mixture was maintained at 80˚C for 2hr under slow stirring. This time was necessary to complete the reaction between metal salts and transformation of hydroxides into a spinel ferrite that dehydration and atomic formation were involved. Then transferred to a beaker and cooled in room temperature for about one hour. The dark precipitate was washed by ethanol and water several times, and then separated by using centrifugation and dried at 65˚C for 24hr. the dark color formed precipitate was calcinated under nitrogen atmosphere at 500˚C for 5hr. Determination and adjusting of pH were carried out with multimeter analyzer PTR79 (Zag chem, Iran).

The structural characteristic and crystalline phase of synthesized manganese ferrite nanocatalyst was recorded by powder X-ray diffractometer. Determinations of surface morphology of nanocatalyst were carried out with field emission scanning electron microscopy (FE-SEM) and an energy dispersive spectroscopy (EDS). The Vibrating Sample Magnetometer (VSM) was used for the measurement of the basic magnetic properties of the manganese ferrite.

### *2.3. Fenton and ElectroFenton Procedure*

The heterogeneous Fenton process was performed in a 100 mL pyrex vessel. In order to perform the process, after adjusting the temperature on 45˚C, 4-cholorophenol solution was poured in to the reactor and its pH was adjusted by $H_2SO_4$ and NaOH. Based on the designed experiments by the software, a known amount of hydrogen peroxide and catalyst were added into the solution. After a certain time of the process, sampling was performed and they analyzed spectrophotometrically. In the next section to perform electro-Fenton process a cylindrical vessel with a 200 mL volume was used. The reactor was equipped with two cast iron electrodes with dimension of 1 ×25 ×150 mm. The electrodes were placed in the center of the reactor with 15 mm distance. Stirring of the solution was performed by a magnetic stirrer. A DC power supply (Shenzen-Masteck, V = 0-50 volt, I = 0-5 A, China) was used as electrical source. In order to perform the Electro-Fenton experiments, 4-cholorophenol solution was poured into the reactor. After adjusting of the solution pH, a known amount of sodium sulfate as supporting electrolyte was added in to the solution and the reaction was started by turning on power supply by using 25volt electric potential. Sampling was performed at regular time and the samples were analyzed by spectrophotometry and TOC analyze (TOC meter (multi N/C3000)).

In this study different variables such as dose of catalyst and $H_2O_2$, concentration of 4-chlorophenol, processing time and pH were examined. The colorimetric method, which recommended by Standard Methods was used to determination of 4-chlorophenol concentration [37]. According to mentioned method, 2.5ml of $NH_4OH$ solution were added to sample. Next with phosphate buffer, pH adjusted at 7.9±0.1. Afterwards, 1ml of 4-Aminoantipyrine and 1ml of $K_3Fe\ (CN)_6$ added respectively and shacked it to yellow color is appeared. Enough time is required to the reaction among reagents were be performed and formation of target complex completed. At the end, concentration of 4-chlorophenol determined with Jasco UV–Vis spectrophotometer model V-530 (Jasco, Japan) At 280 Nm wavelength [38]. The efficiency of the process was defined as follow:

$$\text{Removal Efficiency} = \frac{C_0 - C_e}{C_0} \times 100 \qquad (7)$$

Where $C_0$ is the initial concentration of 4-chlorophenol and $C_e$ is the equilibrium concentration of 4-chlorophenol after Fenton like process

### *2.4. Central Composite Design (CCD) model*

Optimization of physical parameters for maximum degradation was carried out by using response surface methodology, a statistical procedure that is commonly used as a tool to check the efficiency of several processes. Central composite design was used to optimize the process. Based on the CCD method for Five-factors, 26 experiments were performed in in this study. The independent variables studied were $H_2O_2$ dose($X_1$), catalyst dose ($X_2$), pH ($X_3$), contact time ($X_4$) and initial 4-chlorophenol concentration ($X_5$). The response (dependent variable) was removal (R %). Each independent variable was studied at five coded levels (-α, -1, 0, +1, +α). The range of each independent variable and the designed experiment with respect to their coded and un-coded levels are presented in Table 1.

The Central Composite Design used to analyze the data was developed by Design of Experiment software, version 7.0 (Stat-Ease, USA). Data analysis was carried out and the software determined the relationship between the dependent variable and the independent variables [39] and their equation as follows:

$$y = \beta_0 + \sum_{i=1}^{k} \beta_i x_i + \sum_{i=1}^{k} \sum_{j=2}^{k} \beta_{ij} x_i x_j + \sum_{i=1}^{k} \beta_{ii} x_i^2 + \varepsilon \qquad (8)$$

Where Y is the predicted response; $b_0$, $b_i$, $b_{ii}$, $b_{ij}$ are fixed regression coefficients of the model; $X_i$ and $X_j$ represents independent variables.

## 3. RESULTS AND DISCUSSION

### *3.1. Characterization of manganese ferrite nanoparticles*

The FESEM image of the prepared manganese ferrite nanoparticles was shown in Fig 2(a), which reveals the porous structure of this material. This structure effectively increases surface sites for adsorption. Particles with the diameter of 20–60 nm are observed in Fig. 2a.

The EDS spectra of the manganese ferrite nanoparticles are presented in Fig. 2b in order to investigate their localized elemental information. Fe, O and Mn are the dominant elements throughout the surface of manganese ferrite nanoparticles with weight percentages of 47.20, 28.40 and 24.40%, respectively.

The patterns of X-ray powder diffraction (XRD) of the manganese ferrite nanoparticles (JCPDS, 73-1964) are shown in Fig. 2c. The patterns showed that the peaks at 2θ of (1 1 1), (2 2 0), (3 1 1), (1 1 3), (4 0 0), (4 2 2), (5 1 1), (4 4 0), (5 3 1), (5 3 3), (6 2 2) and (4 4 4) are related to single phase $MnFe_2O_4$ with a face-centered cubic structure. The peak at 113 is related to the formation of the α-$Fe_2O_3$ phase which verifies the transfer of $Fe^{3+}$ ions in the mixed spinel structure of $MnFe_2O_4$ nanoparticles [40]. The magnetization curve of the synthesized manganese ferrite is shown in Fig. 2d which was measured at room temperature in range of approximately –10 to +10 kOe, which reveal super-paramagnetic behaviors.

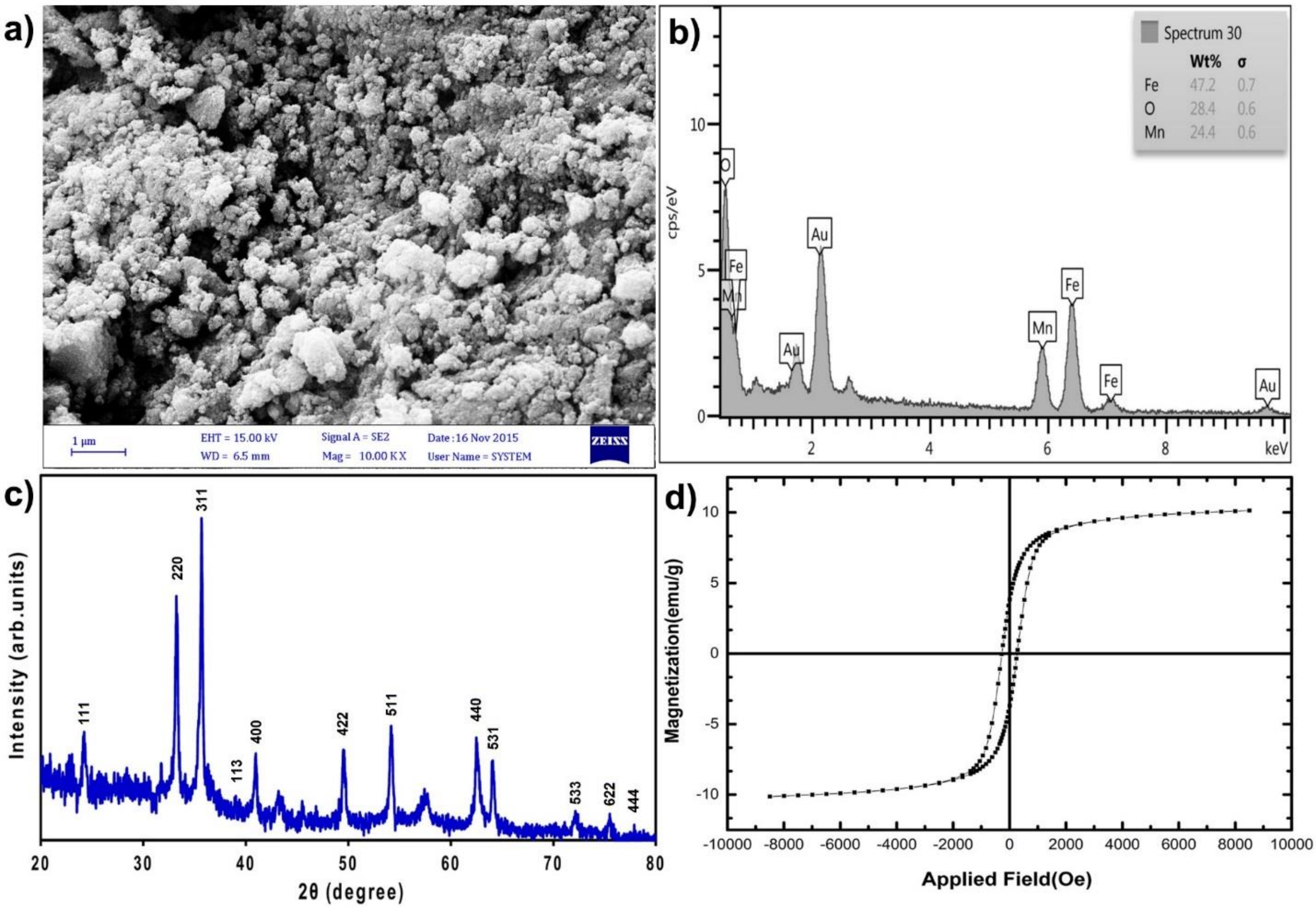

**Figure 2.** a) FE-SEM image, (b) EDS spectrum, (c) XRD patterns and (d) VSM curves of manganese ferrite nanoparticles

### *3.2. Response surface methodology*

The removal of the 4-chlorophenol was optimized through RSM approach. The twenty sex designed experiments for optimizing the five individual parameters in the current CCD were shown in Table 1, and five replicates (runs 22–26) at the center of the design were estimated by a pure error sum of squares [41].

**Table 1**. Coded, actual levels and the experimental observed and predicted responses used in the experimental design

| Factors | unit | Levels | | | | |
|---|---|---|---|---|---|---|
| | | -α | Low (-1) | Central (0) | High (+1) | +α |
| A: $H_2O_2$ dosage | Mole.L$^{-1}$ | 0.025 | 0.04375 | 0.0625 | 0.08125 | 0.1 |

| | | | | | | |
|---|---|---|---|---|---|---|
| B: Catalyst | $g.L^{-1}$ | 0.2 | 0.65 | 1.1 | 1.55 | 2.0 |
| C: pH | - | 3 | 4 | 5 | 6 | 7 |
| D: Contact time | min | 1 | 23.25 | 45.5 | 67.75 | 90 |
| E: 4-chlorophenol Concentration | $Mg.L^{-1}$ | 5 | 22.5 | 40 | 57.5 | 70 |

| | Factors | | | | | R% 4-chlorophenol | |
|---|---|---|---|---|---|---|---|
| Run | A | B | C | D | E | Observed | Predicted |
| 1 | 0.08125 | 1.55 | 2.8 | 67.75 | 22.5 | 55.63 | 55.759 |
| 2 | 0.08125 | 0.65 | 4.4 | 67.75 | 22.5 | 85.32 | 85.449 |
| 3 | 0.04375 | 1.55 | 4.4 | 23.25 | 57.5 | 35.24 | 35.369 |
| 4 | 0.08125 | 1.55 | 4.4 | 23.25 | 22.5 | 69.24 | 69.369 |
| 5 | 0.08125 | 1.55 | 2.8 | 23.25 | 57.5 | 64.36 | 64.489 |
| 6 | 0.08125 | 0.65 | 2.8 | 67.75 | 57.5 | 63.26 | 63.389 |
| 7 | 0.04375 | 0.65 | 4.4 | 67.75 | 57.5 | 49.35 | 49.479 |
| 8 | 0.04375 | 1.55 | 2.8 | 67.75 | 57.5 | 60.25 | 60.379 |
| 9 | 0.08125 | 0.65 | 4.4 | 23.25 | 57.5 | 65.28 | 65.409 |
| 10 | 0.04375 | 1.55 | 4.4 | 67.75 | 22.5 | 41.36 | 41.489 |
| 11 | 0.04375 | 0.65 | 2.8 | 23.25 | 22.5 | 46.65 | 46.907 |
| 12 | 0.02500 | 1.1 | 3.6 | 45.5 | 40 | 34.7 | 34.507 |
| 13 | 0.10000 | 1.1 | 3.6 | 45.5 | 40 | 76.75 | 76.557 |
| 14 | 0.0625 | 0.2 | 3.6 | 45.5 | 40 | 67.15 | 66.957 |
| 15 | 0.0625 | 2.0 | 3.6 | 45.5 | 40 | 46.2 | 46.007 |
| 16 | 0.0625 | 1.1 | 2 | 45.5 | 40 | 47.19 | 46.997 |
| 17 | 0.0625 | 1.1 | 5.2 | 45.5 | 40 | 70.3 | 70.107 |
| 18 | 0.0625 | 1.1 | 3.6 | 1 | 40 | 28.14 | 27.947 |
| 19 | 0.0625 | 1.1 | 3.6 | 90 | 40 | 69.14 | 68.947 |
| 20 | 0.0625 | 1.1 | 3.6 | 45.5 | 5 | 93.24 | 93.047 |
| 21 | 0.0625 | 1.1 | 3.6 | 45.5 | 75 | 54.32 | 54.127 |
| 22 | 0.0625 | 1.1 | 3.6 | 45.5 | 40 | 64.15 | 64.469 |
| 23 | 0.0625 | 1.1 | 3.6 | 45.5 | 40 | 64.25 | 64.469 |
| 24 | 0.0625 | 1.1 | 3.6 | 45.5 | 40 | 64.81 | 64.469 |
| 25 | 0.0625 | 1.1 | 3.6 | 45.5 | 40 | 64.7 | 64.469 |
| 26 | 0.0625 | 1.1 | 3.6 | 45.5 | 40 | 64.05 | 64.469 |

The analysis of variance (ANOVA) for the fitted quadratic polynomial model of removal of 4-chlorophenol is shown in Table 2. The ANOVA analysis was carried out such that p-value less than 0.05 imply the model terms are significant and the values greater than 0.10 imply they are not significant [41]. The P-Value of the model less than 0.0001 implies the model is significant. The regression coefficient for the model is $R^2$ = 0.99981 which suggests that the model could predict 99.98% of the response value changes. Meanwhile, a low value 0.02 of coefficient of the variation (C.V.) implies a high degree of precision and a good deal of reliability of the experimental value. The statistical parameters revealed that the model was adequate to represent the relationship between the response and the independent variables. Furthermore, the lack of fit presents the sufficiency of the fit. The F-value of 5.45 and p-value of 0.0797 represented that the lack of fit was insignificantly to the pure error. Figure 3 shows the correlation between the actual and predicted efficiency values for the degradation of 4-chlorophenol by manganese ferrite catalyst. This plot proves a good fit and existence of high correlation coefficient linear relationship between them. It is seen in figure 4, that the fitted model is appropriate because the errors distributed normally around the mean [41].

**Table 2.** Analysis of variance (ANOVA), regression coefficients and quadratic summary statistics for CCD

| Source | Sum of Square | Degree of Freedom | Mean Square | F-value | P-value | Status |
|---|---|---|---|---|---|---|
| Model | 5810.662 | 20 | 290.5331 | 1321.067 | < 0.0001 | Significant |
| A | 884.1013 | 1 | 884.1013 | 4020.048 | < 0.0001 | |
| B | 219.4513 | 1 | 219.4513 | 997.8547 | < 0.0001 | |
| C | 267.0361 | 1 | 267.0361 | 1214.225 | < 0.0001 | |
| D | 840.5 | 1 | 840.5 | 3821.791 | < 0.0001 | |
| E | 757.3832 | 1 | 757.3832 | 3443.855 | < 0.0001 | |
| AB | 23.08589 | 1 | 23.08589 | 104.9726 | 0.00015 | |
| AC | 1.922471 | 1 | 1.922471 | 8.741561 | 0.031642 | |
| AD | 282.7937 | 1 | 282.7937 | 1285.876 | < 0.0001 | |
| AE | 218.038 | 1 | 218.038 | 991.4288 | < 0.0001 | |
| BC | 41.60323 | 1 | 41.60323 | 189.1717 | < 0.0001 | |
| BD | 89.06709 | 1 | 89.06709 | 404.992 | < 0.0001 | |
| BE | 815.2571 | 1 | 815.2571 | 3707.011 | < 0.0001 | |
| CD | 443.9379 | 1 | 443.9379 | 2018.605 | < 0.0001 | |
| CE | 13.52027 | 1 | 13.52027 | 61.47729 | 0.000542 | |
| DE | 36.29613 | 1 | 36.29613 | 165.0401 | < 0.0001 | |
| $A^2$ | 136.5713 | 1 | 136.5713 | 620.9958 | < 0.0001 | |
| $B^2$ | 109.0803 | 1 | 109.0803 | 495.9929 | < 0.0001 | |
| $C^2$ | 59.8676 | 1 | 59.8676 | 272.2207 | < 0.0001 | |
| $D^2$ | 438.933 | 1 | 438.933 | 1995.848 | < 0.0001 | |
| $E^2$ | 142.1429 | 1 | 142.1429 | 646.3303 | < 0.0001 | |
| Residual | 1.099615 | 5 | 0.219923 | | | |
| Lack of Fit | 0.634335 | 1 | 0.634335 | 5.453364 | 0.079793 | Not significant |
| Pure Error | 0.46528 | 4 | 0.11632 | | | |
| Cor Total | 5811.762 | 25 | | | | |
| **Quadratic summary statistics** | | $R^2$ | Adj-$R^2$ | Pred-$R^2$ | Std. Dev. | C.V. % |
| Response (R %) | | 0.99981 | 0.99905 | 0.93844 | 0.46896 | 0.78917 |

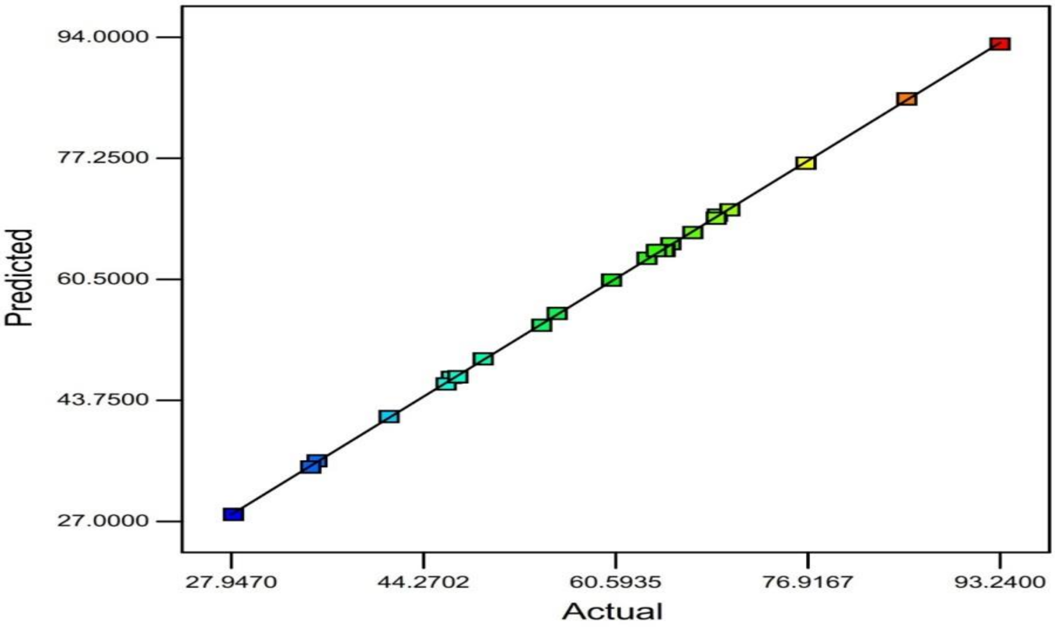

**Figure 3.** Correlation of actual and predicted removal efficiency for 4-chlorophenol

Regression analysis on the experimental data, showed that the following second-order polynomial equation can be modeled the process:

$$R\% = -117.1 + 1234.2A - 25.83B + 50.48C + 5.4D - 5.8E + 309.3AB - 40.2AC - 21.9AD + 24.4AE - 7.8BC - 0.52BD + 1.97BE - 0.52CD + 0.12CE + 0.008DE - 6355.4A^2 - 9.87B^2 - 1.5C^2 - 0.008D^2 + 0.007E^2 \quad (9)$$

Where A, B, C, D and E were the coded $H_2O_2$ dosage (mole. $L^{-1}$), catalyst dose (g.$L^{-1}$), pH, contact time (min) and initial 4-chlorophenol concentration (mg. $L^{-1}$), respectively.

### *3.3. Effect of operational factors and process optimization*

3D plots were used to investigate the effect of operational factors on the process of 4-cholorophenol removal. It is notable that in these plots the effect of two variables is studied while the other parameters are fixed [42]. The effect of pH solution and catalyst dosage on the removal efficiency is shown in Fig 4-A).

pH value has a predominant effect on Hydroxyl free radicals production in Fenton process at alkaline and acidic pH [43]. As can be seen from the figure in the pH rage of 4-6 there is no considerable changes in removal efficiency. Based on the results, degradation efficiency of 4-chlorophenol in near neutral acidic condition (pH=4.24) is higher than that of alkaline condition. This could be due to insufficient and slow decomposition of $H_2O_2$ to high potential hydroxyl radicals (´OH) in lower pH level and also decreasing the oxidation potential of hydroxyl radical in alkaline condition [44, 45]. Fig. 4-B shows the effect of pH and hydrogen peroxide concentration on the removal efficiency. The figure demonstrates that the removal efficiency is increased with increasing of the hydrogen peroxide concentration. This trend is due to hydrogen peroxide is precursor of hydroxyl radicals so removal efficiency will be increased by increasing the concentration of hydrogen peroxide [46, 47]. The effect of time and pH also hydrogen peroxide and catalyst dosage on the removal efficiency were demonstrated in Fig. 4-C and D respectively. Reaction time is also an important factor which has direct effect on size of the reactors and overall cost of treatment process. As can be seen from the figure removal efficiency increased with passing time. The removal efficiency has improved with passing time to about 60 min of the reaction time, but kept almost that level after 60 min. As demonstrated in the figure 4-D increasing catalyst dosage increased removal efficiency due to production of hydroxyl radical from hydrogen peroxide is performed by catalyst [48].

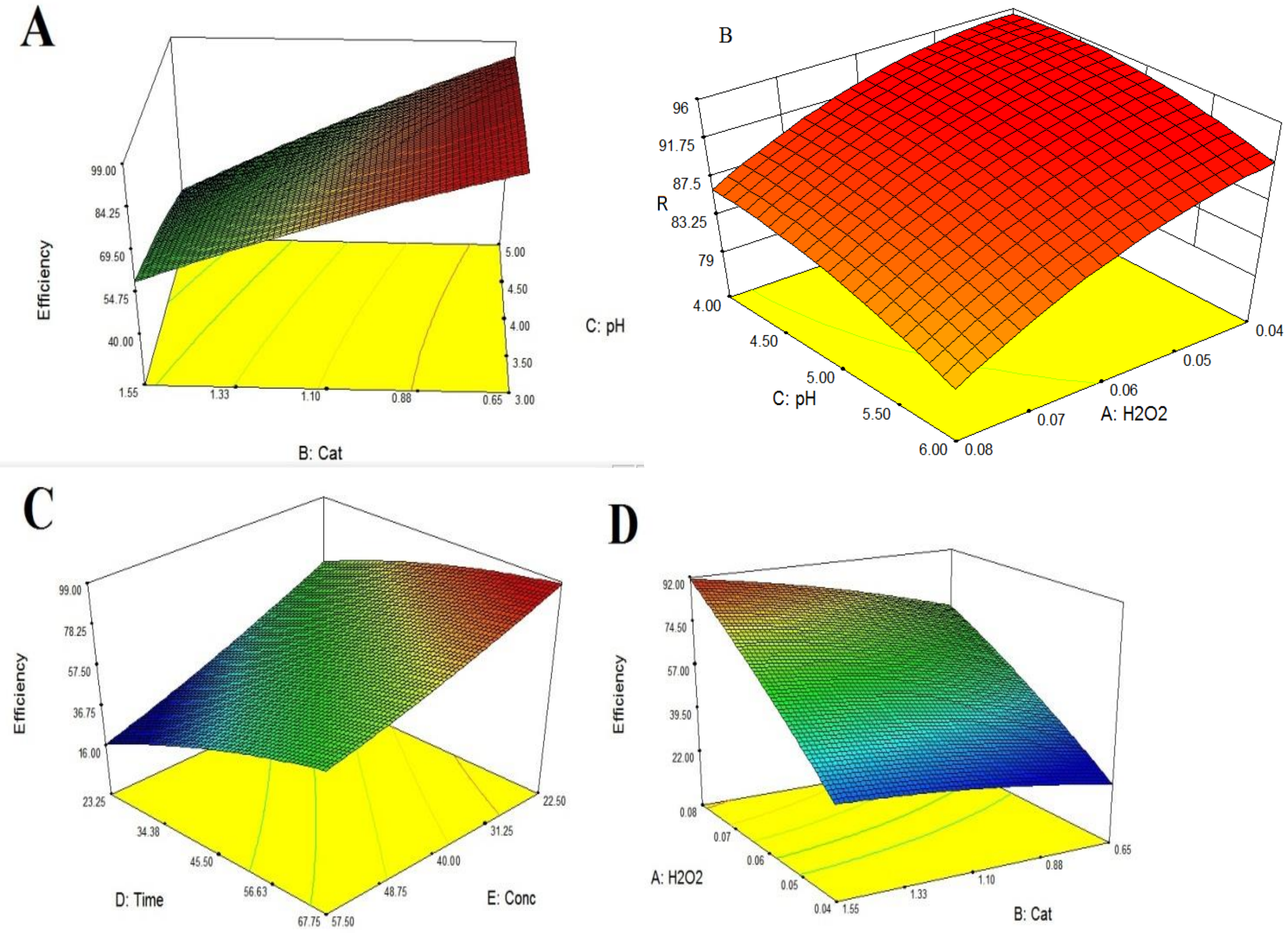

**Figure 4.** 3D plots of the effect of variable on the process efficiency.

Optimization of the process was performed based on the RSM model by the desirability functions as a numerical tool of the software. To this aim the goals of operating variables were set “in the range” and the goal of response was set at maximum also the importance of the response was adjusted in the levels 5. Optimum condition predicted by software was schematically demonstrated in Fig. 5. As can be seen the software predicted 93.27% removal efficiency at the optimum condition of $H_2O_2$ = 0.07 mole. $L^{-1}$, catalyst dosage of 0.72 g. $L^{-1}$, pH = 4.24, and 4-cholorophenol initial concentration of 23.11 $mg.L^{-1}$ after about 61 min of the process time. The model accuracy was performed at optimum condition and 93.27% removal efficiency was obtained.

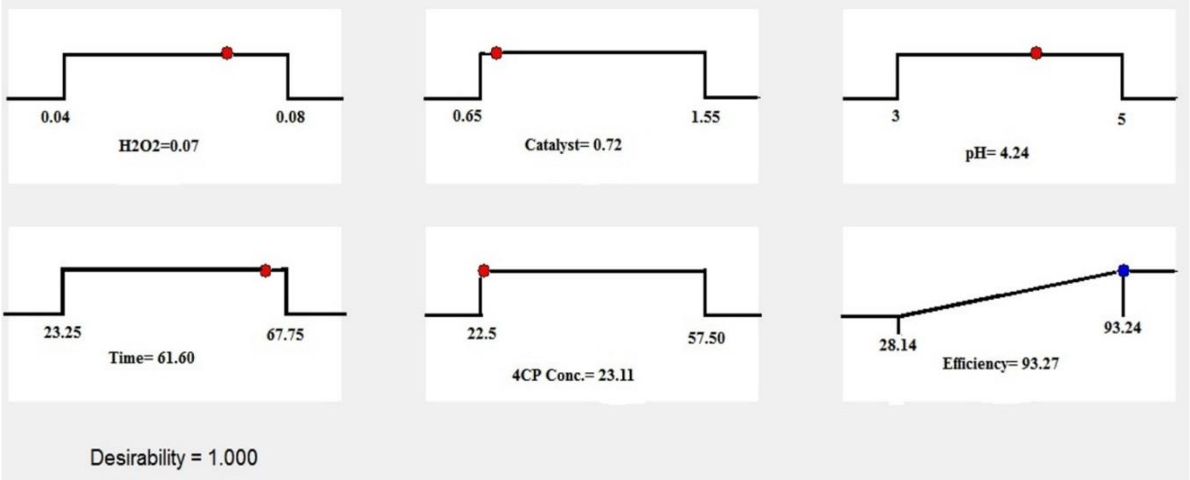

**Figure 5**. Schematic view of the optimum condition

### *3.4. Electro Fenton process*

In order to investigate synergistic effect and compare the results of heterogeneous Fenton and electro-Fenton processes some experiments were performed according to the obtained optimum condition. To this aim an experiment was conducted in the optimum condition, the results showed that 93 and 46% of degradation and TOC removal were obtained in Fenton process. In the next step ElectroFenton process was investigated, one-time hybrid with heterogeneous Fenton and once ElectroFenton lonely at the optimum condition using 25 volt of electric potential. The samples were analyzed by spectroscopy and TOC that the results were demonstrated in Fig. 6. According to the results when the hybrid process of heterogeneous Fenton and ElectroFenton were performed degradation and mineralization efficiency are further. The addition of manganese ferrite nanocatalyst and $H_2O_2$ to ElectroFenton cell can accelerate the generation of hydroxyl radicals and also a greater amount of the hydroxyl radical production, this lead to further degradation of 4-chlorophenol [19, 49, 50]. Also it is shown that the heterogeneous Fenton process efficiency is greater than ElectroFenton process. According to the experiments results, total organic carbon removal (TOC) in hybrid process is higher than ElectroFenton and heterogeneous Fenton. As can be seen in figure 6, 53% of TOC was removed in 60 minutes and 55.3% in 90 minutes' treatment time in hybrid process. The removal amount of TOC in heterogeneous Fenton and ElectroFenton was 46% and 35.5% in 60 minutes' reaction time of process, respectively. Higher 4-chlorophenol and TOC removal efficiency in hybrid process can be attributed to the increasing in $Fe^{2+}$, $Mn^{2+}$ ions and $OH^{\circ}$ reactive radicals amount due to the addition of manganese ferrite and $H_2O_2$ to the electrochemical reactor, which can enhance the 4-chlorophenol degradation rate [19, 51].

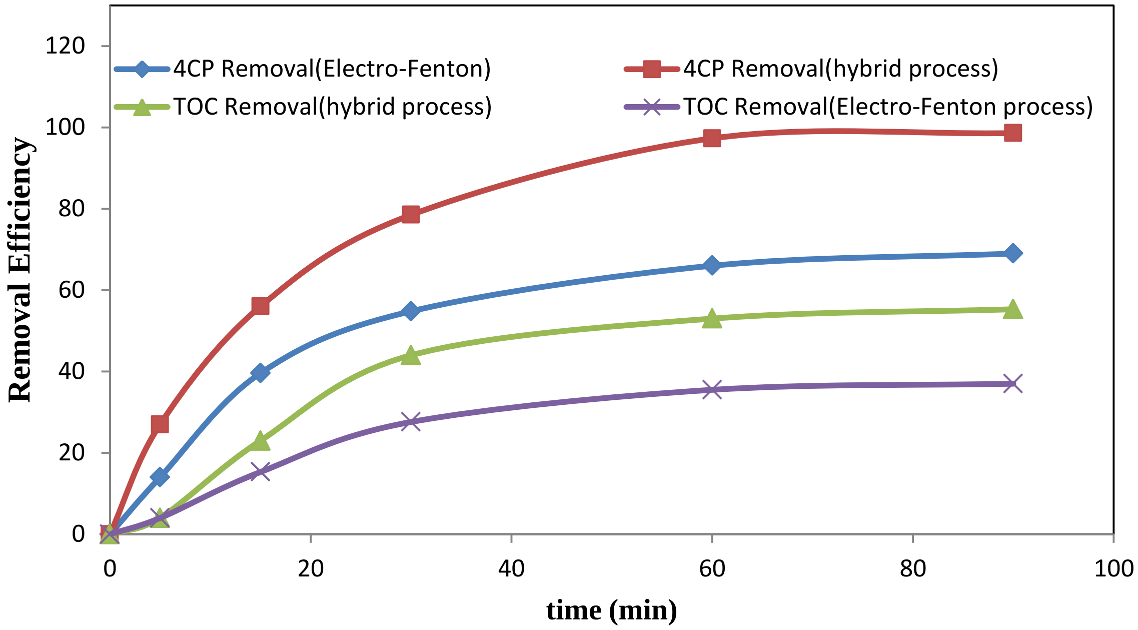

**Figure 6.** Removal efficiency of electro-Fenton process in hybrid by heterogeneous Fenton and lonely

## 4. CONCLUSIONS

In this study, we investigated effective parameter on catalytic degradation of 4-chlorophenol. For this purpose, manganese ferrite nanomaterial synthesized and characterized and used for oxidation of pollutant in Fenton process.

Based on the results of characterization analysis, XRD data of synthesized $MnFe_2O_4$ proof crystalline phase composition and FE-SEM data show prose composition which could increase active site for catalytic process. The effect of operating parameters such as reaction time, catalyst dose, hydrogen peroxide and 4-chlorophenol concentration and pH on the degradation efficiency of oxidation process explored from experiment results. Based on the results and fitted model, the optimum level of pH, hydrogen peroxide concentration and catalyst dose were 4.24, 0.07 mole per liter and 0.72 gram per liter respectively. Also, optimum initial 4-chlorophenol concentration was 23.11mgL$^{-1}$ at 61 min reaction time studied to achieve the maximum degradation efficiency (93%). Results of experiments showed that use of the manganese ferrite as catalyst in Fenton process for catalytic degradation of 4-chlorophenol was rapid and effective. Also comparison of the electro-Fenton and heterogeneous Fenton processes showed that the heterogeneous Fenton process has better result. But 4-chlorophenol degradation and TOC removal efficiency in hybrid process were higher than Fenton and ElectroFenton process efficiency.

ACKNOWLEDGEMENT

This research was part of PhD thesis of Ghasem Hassani, an environmental health engineering student in Ahvaz Jundishapur University of Medical Sciences (AJUMS). The authors sincerely thank the

Environmental Technologies Research Center (ETRC), Ahvaz Jundishapur University of Medical Sciences for financial support of this study (grant No.: ETRC-9418).

*Conflicts of Interest*
The authors declare no conflict of interest.

## References

1. L.H. Keith, *Pure Appl. Chem*., 70 (1998) 2319.
2. A. Kuleyin, *J. Hazard. Mater.*, 144 (2007) 307.
3. B. Kakavandi, M. Jahangiri-rad, M. Rafiee, A.R. Esfahani, and A.A. Babaei, *Microporous Mesoporous Mater*., 231 (2016) 192.
4. H. Godini, F. Hashemi, L. Mansuri, M. Sardar, G. Hassani, S. Mohseni, A. Alinejad, S. Golmohammadi, and A.S. Mohammadi, J*ournal of Water Reuse and Desalination*, (2016) jwrd2016068.
5. O. Hamdaoui and E. Naffrechoux, *J. Hazard. Mater.,* 147 (2007) 381.
6. M.S. Bilgili, *J. Hazard. Mater*., 137 (2006) 157.
7. B. Hameed, L. Chin, and S. Rengaraj, *Desalination*, 225 (2008) 185.
8. J. Fan, J. Zhang, C. Zhang, L. Ren, and Q. Shi, *Desalination,* 267 (2011) 139.
9. B. Hameed, I. Tan, and A. Ahmad, *J. Hazard. Mater.*, 164 (2009) 1316.
10. W. Jianlong, Q. Yi, N. Horan, and E. Stentiford, *Bioresour. Technol*., 75 (2000) 157.
11. R. Cheng, J.-l. Wang, and W.-x. Zhang, *J. Hazard. Mater.*, 144 (2007) 334.
12. H. Wang and J. Wang, *Appl. Catal. B*, 77 (2007) 58.
13. S. Chaliha and K.G. Bhattacharyya, *Chem. Eng. J.*, 139 (2008) 575.
14. P. Saritha, D.S.S. Raj, C. Aparna, P.N.V. Laxmi, V. Himabindu, and Y. Anjaneyulu, *Water, Air, Soil Pollut.*, 200 (2009) 169.
15. C.G. Joseph, G.L. Puma, A. Bono, Y.H. Taufiq-Yap, and D. Krishnaiah, *Desalination,* 276 (2011) 303.
16. J. Hu and J. Wang, *Radiat. Phys. Chem*., 76 (2007) 1489.
17. A.R. Zarei, H. Rezaeivahidian, and A.R. Soleymani, *Process Saf. Environ. Pro*t., 98 (2015) 109.
18. A. Babaei, A. Mesdaghiniai, N.J. Haghighi, R. Nabizadeh, and A. Mahvi, *J. Hazard. Mater*., 185 (2011) 1273.
19. J.L. Wang and L.J. Xu, *Crit. Rev. Environ. Sci. Technol.*, 42 (2012) 251.
20. Y. Song-Hu and L. Xiao-Hua, *J. Hazard. Mater*., 118 (2005) 85.
21. K. Swaminathan, S. Sandhya, A.C. Sophia, K. Pachhade, and Y. Subrahmanyam, *Chemosphere*, 50 (2003) 619.
22. W.Z. Tang and R.Z. Chen, *Chemosphere*, 32 (1996) 947.
23. W. Bae, S. Lee, and G. Ko, *Water Sci. Technol*., 49 (2004) 91.
24. H. Fenton, *J. Chem. Soc., Trans*., 65 (1894) 899.
25. L.G. Devi, S.G. Kumar, K.M. Reddy, and C. Munikrishnappa, *J. Hazard. Mater.*, 164 (2009) 459.
26. Z.-R. Tang, *Green catalysts preparation using supercritical CO2 as an antisolvent*. 2007, Cardiff University.
27. S. Jauhar and S. Singhal, *Ceram. Int*., 40 (2014) 11845.
28. A. Wang, J. Qu, J. Ru, H. Liu, and J. Ge, *Dyes. Pigments.*, 65 (2005) 227.
29. E. Brillas, I. Sirés, and M.A. Oturan, *Chem. Rev*., 109 (2009) 6570.
30. M. Pimentel, N. Oturan, M. Dezotti, and M.A. Oturan, *Appl. Catal. B*, 83 (2008) 140.
31. S.S. Martínez and C.L. Bahena, *Water Res*., 43 (2009) 33.
32. E. Isarain-Chávez, C. De La Rosa, C.A. Martínez-Huitle, and J.M. Peralta-Hernández, *Int. J. Electrochem. Sci.*, 8 (2013) 3084.

33. X. Xu, J. Chen, G. Zhang, Y. Song, and F. Yang, Int. *J. Electrochem. Sci,* 9 (2014) 569.
34. M. Kooti and M. Afshari, *Sci. Iranica*, 19 (2012) 1991.
35. S. Zhang, H. Niu, Y. Cai, X. Zhao, and Y. Shi, *Chem. Eng. J.*, 158 (2010) 599.
36. Y. Zhou, B. Xiao, S.-Q. Liu, Z. Meng, Z.-G. Chen, C.-Y. Zou, C.-B. Liu, F. Chen, and X. Zhou, *Chem. Eng. J.*, 283 (2016) 266.
37. L.S. Clesceri, A.E. Greenberg, A.D. Eaton, E.W. Rice, and M.A.H. Franson, *Standard methods for the examination of water and wastewater*. 1995, American Public Health Association: washington, DC. p. 36.
38. E. Rubín, P. Rodríguez, R. Herrero, S. de Vicente, and E. Manuel, *J. Chem. Technol. Biotechnol.*, 81 (2006) 1093.
39. S.S. Chong, A.A. Aziz, S.W. Harun, H. Arof, and S. Shamshirband, *Measurement,* 74 (2015) 78.
40. M.G. Naseri, E.B. Saion, H.A. Ahangar, M. Hashim, and A.H. Shaari, *J. Magn. Magn. Mater.*, 323 (2011) 1745.
41. J. Wu, D. Yu, H. Sun, Y. Zhang, W. Zhang, F. Meng, and X. Du, *Ind Crops Prod*, 69 (2015) 68.
42. F.N. Azad, M. Ghaedi, K. Dashtian, A. Jamshidi, G. Hassani, M. Montazerozohori, S. Hajati, M. Rajabi, and A. Bazrafshan, *RSC Advances*, 6 (2016) 19780.
43. M. Kitis, C.D. Adams, and G. Daigger, *Water Res*., 33 (1999) 2561.
44. D.L. Sedlak and A.W. Andren, *Environ. Sci. Technol.*, 25 (1991) 777.
45. M. Farrokhi, A. Mesdaghinia, S. Naseri, and A. Yazdanbakhsh, *Iran. J. Public. Health*., 32 (2003) 6.
46. G.V. Buxton, C.L. Greenstock, W.P. Helman, and A.B. Ross, *J. Phys. Chem. Ref. Data*, 17 (1988) 513.
47. S.-S. Lin and M.D. Gurol, *Environ. Sci. Technol.*, 32 (1998) 1417.
48. S.H. Lin and C.C. Lo, *Water Res*., 31 (1997) 2050.
49. H. Kusic, N. Koprivanac, and A.L. Bozic, *Chem. Eng. J.*, 123 (2006) 127.
50. T.-S. Chen, R.-W. Tsai, Y.-S. Chen, and K.-L. Huang, *Int. J. Electrochem. Sci*, 9 (2014) 8422.
51. E. Brillas, E. Mur, R. Sauleda, L. Sànchez, J. Peral, X. Domènech, and J. Casado, *Appl. Catal. B*, 16 (1998) 31.